



The interest of computation to understand dynamic buckling shear experiments

Combescure A.G.
ENS Cachan / LMT, France

ABSTRACT

In this paper we give the results of the computation of the dynamic shear buckling of a cylinder. We try to understand the main physical phenomenon involved by this buckling. For this purpose a detailed vibration analysis is performed and a spectral analysis of the transient response signal is performed. The computed results are rather close to the experimental observations and we conclude, by analysis, that the loading is rather slow to be considered as a dynamic one. The efficiency of the proposed computation allows to help for the interpretation of experimental results by the fabrication of an animation of the computed deformed structures. This film helps a lot to understand the experiments.

1 INTRODUCTION

The prediction of stability of thin structures subjected to seismic type of load is based mainly on static buckling concepts. That is to say: one computes the stress state using dynamic analysis and one uses this "frozen" stress state, as if it were a static one, to evaluate stability. In some cases this method can be conservative (for instance in some case of pulse loadings) but in other cases one can fear that this method is not conservative because for instance it does not take into account parametric resonance phenomena. In order to assess the quality of the design rules used by nuclear industry in case of seismic loading EDF CEA and FRAMATOME have decided to launch an experimental program aimed to simulate seismic buckling of thin cylinders submitted to a seismic shear imposed displacement. This paper describes the theoretical studies performed to define the experiments as well as the comparison between simulations and the first experimental results. The main goal of the paper is to study the influence of the rate of loading on the buckling of the cylinder and also to investigate the role of the initial imperfections on the dynamic shear buckling.

2 GEOMETRY

The geometry was chosen to be representative of a typical fast breeder main vessel. It is a cylinder having a mean radius R of .1245m, a nominal thickness h of 270 microns, and an height H of .125m. One can anyway observe that the shell is rather thin (the R/h ratio being not far from 500) so that this study is also valid for other types of structures like Ariane tanks or typical space structures.

21 nominal

The cylinder is attached at its extremities to two thicker rings. This is to ensure a good quality for the boundary condition at the basis and at the top. The thickness has been measured with great care in all positions.

22 initial imperfections

The shape is measured on about 50 parallels and is decomposed in Fourier series to control and understand the way initial imperfections come into the system. The observed initial imperfection amplitude are rather small (between 10% and to 50% of the thickness). The fabricated specimens can hence be considered as of "good" quality. For the modelisation, we have chosen to take an initial imperfection having the shape of the elastic buckling mode, but with a typical measured amplitude. We have done the nonlinear computations with two amplitudes: the first one of 20 microns, which is hardly measurable, and the second one of 100 microns, corresponding to a mean measured initial imperfection.

3 MATERIAL PROPERTIES

The material properties have been measured during the experiment; we have chosen the following values for the modelisation: the Poisson's ratio is chosen to be .3. The Young's modulus is 180000Mpa. The stress strain curve is given by the following Table 1 in which we define the stress σ as a function of the strain ϵ .

σ (Mpa)	ϵ
180	0,001
300	0,0018
400	0,0027
500	0,0038
600	0,0052
700	0,0075

Table 1 Stress-strain curve chosen for the analysis

The density of the material is 8000Kg/m³.

4 LOADING SYSTEM

The cylinder is loaded in shear by an actuator, which is displacement controlled. In order to transmit the displacement to the shell, a rigid plate is put on the top of the specimen and the cylinder is also screwed on a very thick plate at its base. The top system is rather heavy so that it was decided to hang it to avoid to load the specimen in compression. Anyway the inertia of this heavy mass has to be taken into account for the horizontal motion evaluation. The experimental testing system is represented on Figure 1.

5 BOUNDARY CONDITIONS

The specimen can be considered as clamped at its base, and an horizontal displacement is imposed on the rigid plate at the top of the model. Nevertheless the top plate is free to rotate.

6 MAIN EXPERIMENTAL RESULTS

First the static shear buckling load and the corresponding displacement were measured. The cylinder buckles for a tranverse load of 750daN associated with a tranverse horizontal displacement U_b of 0.15mm.

The eigen frequencies where measured and it was observed that the first mode was close to 80 Hz.

The cylinder was then loaded with an horizontal imposed displacement, periodic in time . Equation (1) gives the chosen time function to impose the displacement.

$$u(t) = um \times \sin(\alpha t) \quad (1)$$

The maximum displacement, um , is chosen larger than the static buckling displacement U_b . A set of experiences was conducted with a set of frequencies starting for 10 Hz up to 50 Hz. The main results obtained can be summarized as follows: buckling has been observed in all cases. The maximum measured load is very close to the static one when the frequency is low but is higher when the frequency increases. The buckling is mainly elastic: one can ipose the cylinder hundreds of cycles without changing significantly its shape. The buckling modes appear at each cycle and dissappear when the imposed displacement is close to 0.

7 CHOICE OF MODELISATION

In order to compute the dynamic behavior of this structure, we have chosen to use a quasi axisymmetric modelisation which allows a good understanding of the dynamic behavior of the shell. With this modelisation we shall have access, during the transient, to the dynamic behavior of all individual Fourier mode that come into the problem. In order to take into account the added masses of the thick top plate, the plate has been meshed.

71 the imperfect COMU shell element

The quasi axisymmetric COMU shell element was chosen to model the problem. Details of the formulation can be found in [1]. This element is a two node flat Mindlin shell element; at each node the geometry is defined by the r, z cordinates, as well as by an initial non axisymmetric displacement. This field defines the initial imperfection and it is given on a set of Fourier circumferencial harmonics, chosen by the analyst. The displacement response is also decomposed in Fourier series: the analyst chooses the appropriate set of Fourier modes for his

analysis. The plasticity is evaluated on discrete points around the circumference and its influence on the equilibrium is computed via a Fourier transform of the plastic strains. The geometrical nonlinearities are modeled by an updated Lagrangian technique: the axisymmetric coordinates are simply updated, whereas the initial imperfections are updated at each time step. This element is implemented in the INCA code of the CASTEM system.

72 The modelisation choices

721 mesh

The test specimen has been meshed with 20 elements. The thicker junctions to the base and to the top have been modelised by 1 element. The top part has been meshed with 8 elements for the plate and 2 for the vertical part.

722 the choice of the Fourier basis

7221 for initial imperfection

For the linear buckling analysis no initial imperfection where chosen. For the nonlinear cases, static or dynamic, the initial imperfection was chosen to be affine to the first elastic buckling mode. In order to have a reasonable computational time, for the transient analyses the imperfection was chosen to be a combination of circonfential modes 14 15 16 17 18. These modes are just sufficient to get a good estimation of the buckling load under shear. Two amplitudes have been chosen for the maximum radius difference. The first one is very small (20 microns) which is the limit of what can be observed experimentally. The second one is chosen to be 100 microns and is larger than all measured initial imperfections.

7222 for displacement response

For the linear buckling analysis we have a mode 1 loading and the buckling analysis was performed with a combination of Fourier modes between 14 and 18 up to between 11 and 23. For the nonlinear response, static or dynamic, and for the vibration analysis we have chosen the following modal basis for the displacements: 0,1,2,14 to 18,28 to 36.

7223 for evaluation of plasticity

We have chosen to put 121 points around the circonference to evaluate plasticity.

8 LINEAR ELASTIC ANALYSIS

81 elastic buckling load and mode

The elastic buckling mode is found to occur for a transverse horizontal displacement of 0.15mm and the corresponding horizontal load is 755daN. We observe on the buckling mode that the mode has a null amplitude on the mid plane of the shell and a maximum amplitude at three quarter of the shell.

This result is obtained as the converged value when one choses enough Fourier modes for the buckling load evaluation. Table 2 summarises the convergence study performed. Finally, we have chosen the basis 14 to 18 to represent the initial imperfection because this is the smallest basis giving an error less than 10% for the elastic buckling load.

modal basis	critical load (daN) (critical mode)
14 to 18	824 (16)
13 to 19	780 (16)
12 to 20	765 (17)
12 to 22	756 (17)
11 to 23	755 (17)

Table 2 convergence study for buckling evaluation

82 eigen frequencies an eigenmode analysis

In order to understand the characteristic times involved in this dynamic buckling problem, a vibration analysis of the structure was done. The present paragraph presents the results obtained by this analysis.

822 influence of initial imperfections

In this paragraph we study the influence of an initial imperfection, of the shape of the buckling mode, on the eigen frequencies and on the eigen modes. We have first studied the influence of the added mass on the perfect cylinder and then have studied the influence of the initial imperfection amplitude.

Table 3 given just below summarizes the results.

imper (μm)	0 added mass											mode type
	0	38 KG added mass										
mode	0	20	100	200	300	400	500	750	1000	2000		
1	231	80	80	79	78	77	75.5	74	70.5	67.1	57	shear mode
2	433	188	188	188	188	187	187	187	185	184	181	torsion mode
3	587	473	473	473	473	473	473	473	473	473	474	axi extension
4	842	839	839	837	834	831	827	825	817	810	791	axial bending
5	943	943	944	975	1035	1079	1104	1125	1175	1226	1431	1rst mode 14
6	1013	1013	1011	1028	1067	1152	1171	1223	1328	1400	1520	1rst mode 15
7	1100	1100	1098	1113	1156	1210	1264	1389	1379	1433	1772	1rst mode 16
8	1200	1200	1202	1218	1268	1341	1420	1485	1577	1637	1830	1rst mode 17
9	1315	1315	1320	1356	1442	1514	1538	1550	1668	1803	2000	1rstmode 18
10	1503	1503	1497	1505	1519	1530	1563	1602	1752	1822	2240	2nd mode 15
11	1515	1515	1511	1517	1529	1551	1596	1662	1810	1954	2400	2nd mode 14
12	1520	1520	1515	1530	1579	1646	1724	1810	1870	1958		2nd mode 16
13	1570	1570	1560	1653	1611	1720	1838	1843	2055	2015		2nd mode 17
14	1640	1640	1630	1842	1741	1830	1860					2nd mode 18

Table 3 influence of initial imperfection on the eigenfrequencies

The first eigen mode of the imperfect shell with an imperfection of 20μ is plotted on Figure 2. The 2nd eigen mode with no imperfection is plotted on Figure 3.

First we observe that the added mass decreases the eigen frequencies of the first four modes which are axisymmetric and mode one type. The other modes, which are shell modes, remain unaffected by the added mass as one could have expected.

Second we remark that an initial imperfection up to one time the thickness has a very small influence on the eigenfrequency but has a significant influence on the modeshape. The modeshapes are all coupled with the deformation associated with the initial imperfection which is amplified by vibration. We can also observe that the initial imperfection mainly influences the modes which contain the initial imperfection. We also observe that when we increase the initial imperfection the eigen-frequency of the modes of the imperfection also increase.

When the initial imperfection is large (about ten times the thickness) the eigen frequency of the first mode decreases of about 25% and the mode shapes associated with the first axial mode for circumferential mode 14 to 18 do not appear any more and are replaced by modes associated with the second axial mode which are the modes corresponding to the initial imperfection.

823 conclusions of the vibrational parametric analysis

We will now use the previous information to try to understand what shall happen when the structure shall deform due to the dynamic loading. The structure shall see two effects: first the initial imperfection shall be amplified, and second the structure shall see stresses induced by the loading. The effect of the instantaneous stress shall be to decrease the instantaneous eigen frequency to zero when the lateral imposed displacement shall reach the critical buckling displacement U_b , if one makes the hypothesis that the stresses in the shell are directly in phase and related to the imposed lateral displacement. This is probably true when the frequency of the applied displacement is small when compared to the frequency of the buckling mode (here about 1500Hz). We think that we are in this case. On the other hand the initial imperfection shall increase due to nonlinear effects and hence the instantaneous eigen-frequencies will be changing: nevertheless the lateral displacements will have to be of the order of ten times the thickness to imply about 20% change in the eigenfrequencies: hence this effect should be minor in our case.

9 NONLINEAR ANALYSIS

We are going to give in this paragraph the results obtained by the nonlinear analysis in the static case as well as in the different dynamic cases performed. For all computations a maximum lateral displacement u_m of 300 microns has been imposed. For all dynamic cases a very small initial imperfection of 20 microns has been taken.

91 static loading comparison with experiment

The nonlinear static analysis has been performed taking into account plasticity. The deformed structure at maximum displacement can be observed on Figure 4. We observe a buckling starting for transverse displacement of 250 Microns. Very similar results are obtained with an initial imperfection of 100μ amplitude; the only difference is the initial slope of the load displacement curve which is smaller with a larger initial imperfection.

92 dynamic loading

Different dynamic computations were performed with different loading frequencies with the very small initial imperfection. The following cases have been studied: 1Hz, 10Hz, 40Hz, 50Hz, 80Hz, 100Hz, 750Hz, 1000Hz, 1500Hz, 2000Hz. All simulations are performed without damping as we think that nonlinearities can kill the divergence. We shall now comment on the solutions and compare with experimental results.

The following Table 4 summarises the main results of the spectral analysis of the radial displacement on mode 16 of the node 17(maximum radial initial imperfection). In this table we give the response frequencies classified by their amplitude. The second column contains the frequency associated with the maximum amplitude of response, the third contains the frequency associated with the second amplitude. This table is interesting and we can draw some conclusions from these numbers.

excitation frequency	first maxi (Hz)	2nd maxi (Hz)
10	10	
40	40	
50	40	120
80	40	120
100	100	200
750	750	1500
1000	1250	1750
1500	1500	750
2000	1250	

Table 4 response spectrum for radial displacement of mode 16

For slow excitation frequencies (less than 100Hz) we observe first that the mode 16 does not respond on 80Hz which is the first eigen frequency of the structure but on multiples of 40Hz which is the half of the first eigen frequency. This is typical of a parametric resonant response which is represented usually by Hill's equation. This type of dynamic nonlinear equation mainly responds to the half frequency of the linear model. The presence of multiples of 40Hz is typical of the nonlinearity of the answer. A typical load time curve is given on Figure 5. A load displacement is given on Figure 6 where we can observe the cyclic shear behavior.

The frequency response to high frequencies excitation is on the multiple of 750Hz (half the frequency of the buckling mode) for an excitation on 750Hz and 1500Hz. For 1000Hz and 2000Hz excitations the response is not on the ecitation frequency but on linear combination of this frequency with the basic high frequency (750Hz).

excitation frequency	experimental Load (daN)	computed Load (daN)	Filter frequency (Hz)
10	720	720	
40	730	720	
50		750	2000
80		800	4000
100		900	5000
750		1200	7500
1000		1500	10000
1500		1900	10000
2000		2200	10000

Table 5 Computed shear reactions compared with experiments

If we now observe the amplitude of the reaction load at the base associated to imposed displacement (Table 5) we can remark that it is nearly constant up to the 100Hz: there is a

small increase with the applied frequency after 80Hz. One can quote that the reaction force does not decrease to 0. when we approach the first eigen frequency (80Hz), as one would expect for the applied load in case of the response of a linear oscillator to an imposed displacement. A future paper, with a one degree of freedom model which represents the geometrical nonlinear behavior of the model, shall show this clearly.

At high frequencies (over 1000Hz) the amplitude of the reaction force is nearly proportionnal to the the ratio of the applied frequency ω to the first eigen frequency ω_1 : we can observe that on Figure 7 (the response is filtered below 20000Hz).

The response of mode 16 is of progressive buckling type as can be seen from Figure 8.

932 comparison with experimental results

The only available experimental results are available up to 40Hz. We observe here a slow loading rate. Globally it has been observed that the dynamic buckling load is close to the static one. This experimental result is very similar to those of the numerical simulations. One can deduce from this comparison that the simulations are in good agreement with experimental results. The computed result for an excitation frequency of 40Hz was also animated and we could observe on the film a lateral vibration, at a frequency of about 1000Hz, occuring when the structure starts to buckle (lateral displacement ub f 250 microns).

10 CONCLUSIONS

In this paper we have reported the comparison of a dynamic shear buckling simulation using the COMU element of the INCA computer tool with an experimental set of results. The comparison is rather good for this case. As in the experiment, we observe that the imposed shear displacement at a frequency less than half the first eigenfrequency lead to a dynamic buckling load close to the static one. This could have been expected, because the eigenfrequency associated with the buckling mode is about 20 times higher than the shear deformation eigen frequency of the shell. Therefore one would expect that the shell responds as if it was loaded statically. The simulations also show a lateral vibration occuring during the buckling: this vibration could not be observed in the experiments; its frequency was too high to be observed with a camera fixing only one thousand images per second. Therefore the simulation is very interesting: it allows now to avoid a lot of experiments and to study in details the movements of all points in the structure. This analysis validates the computing tool and makes it really usefull to design and understand seismic buckling.

REFERENCES

[Combesure 1] A Combesure 1986

Static and dynamic buckling of large thin shells
Nuclear Engineering and design,92,339-354

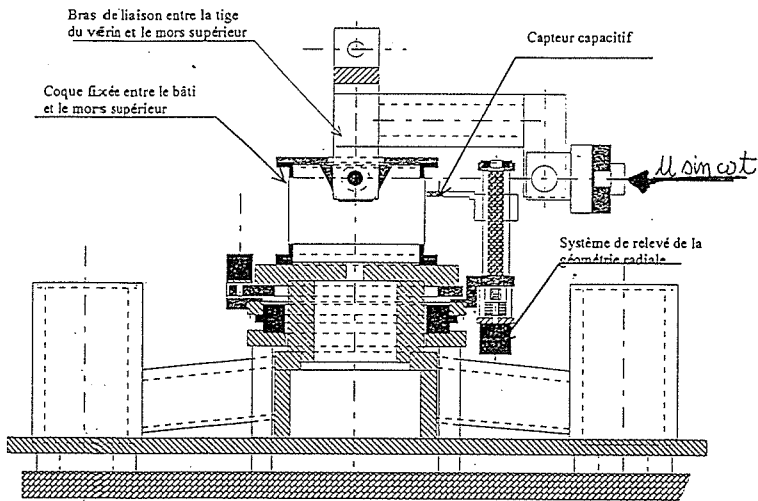


Figure 1 Test rig

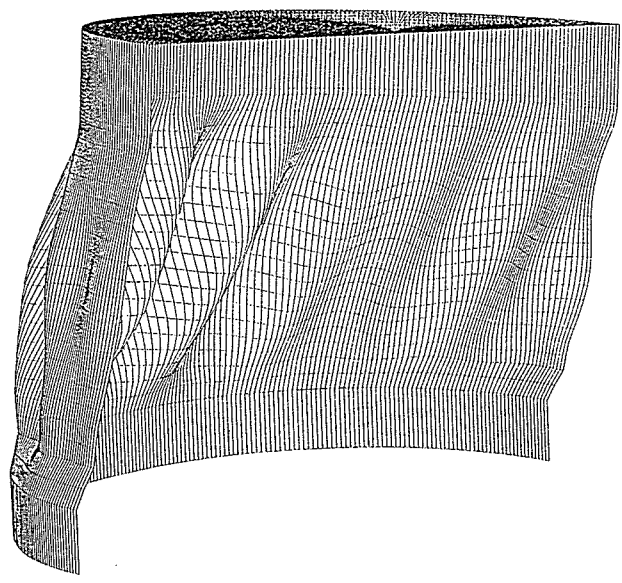


Figure 2 1rst eigenmode initial imperfection 100μ eigen frequency 80Hz

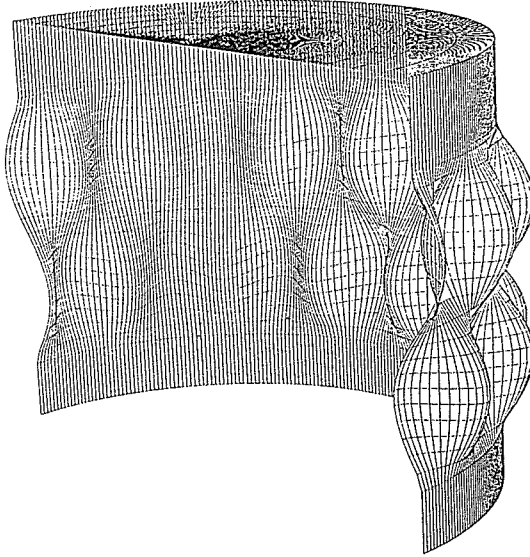


Figure 3 2nd eigen-mode for Fourier mode 14 (1515Hz) no imperfection.

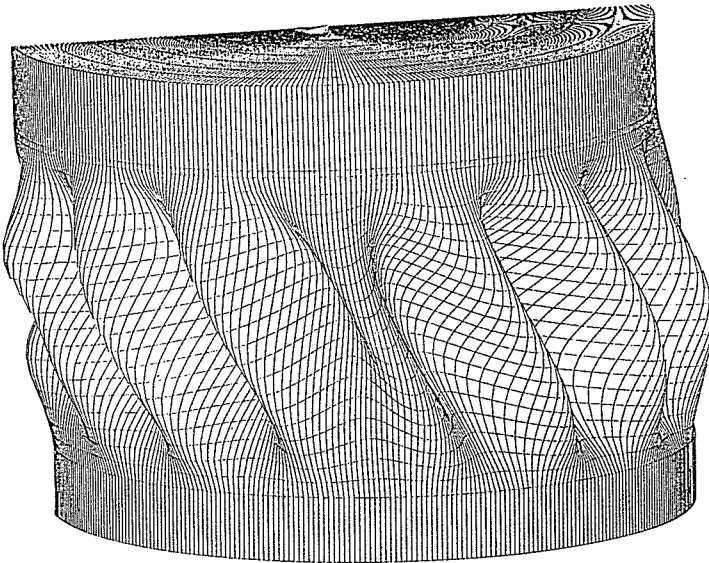


Figure 4 Static nonlinear buckled structure initial imperfection 20μ
lateral displacement 300μ

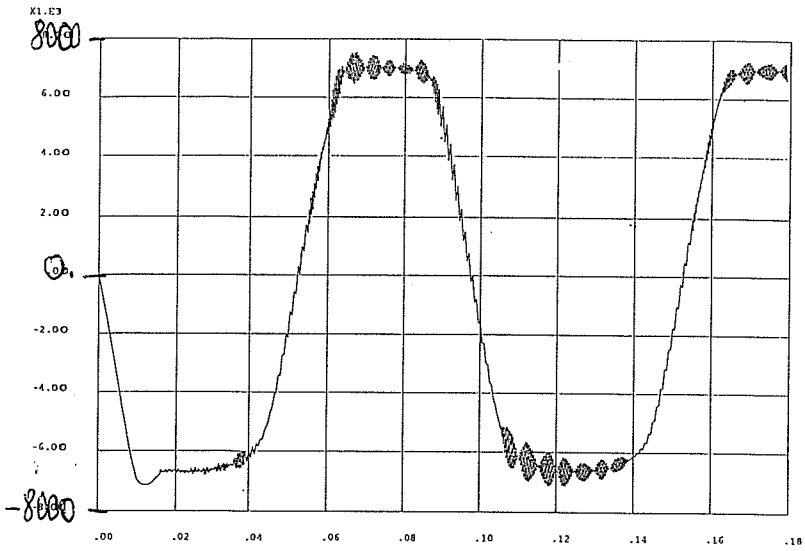


Figure 5 Typical Load-time curve slow excitation (10Hz)

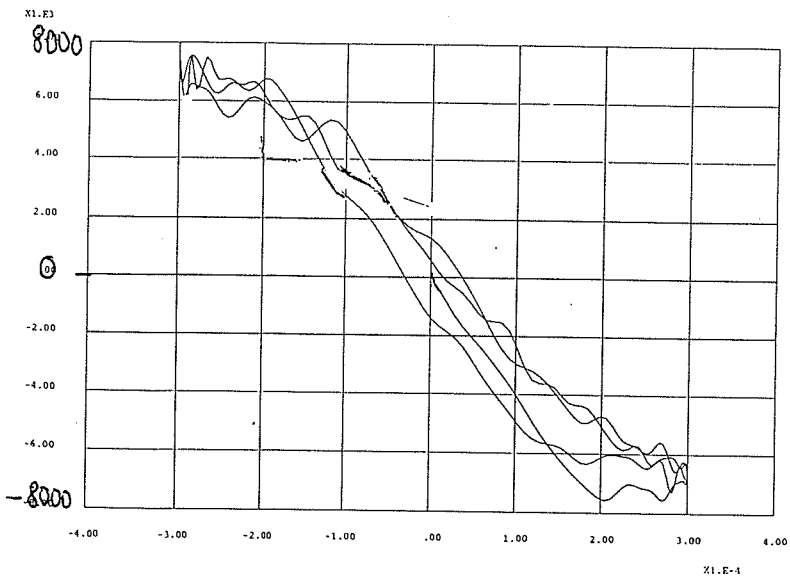


Figure 6 Load displacement curve for a 50Hz excitation

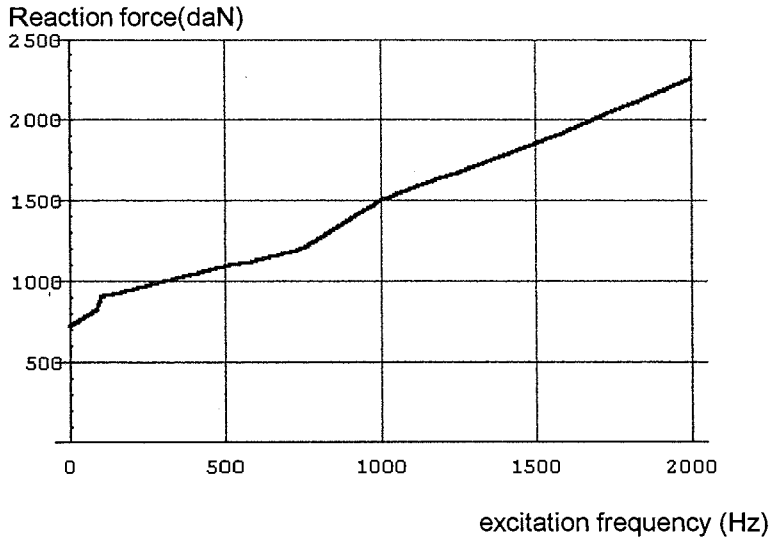


Figure 7 Evolution of reaction force as a function of the excitation frequency (Hz)

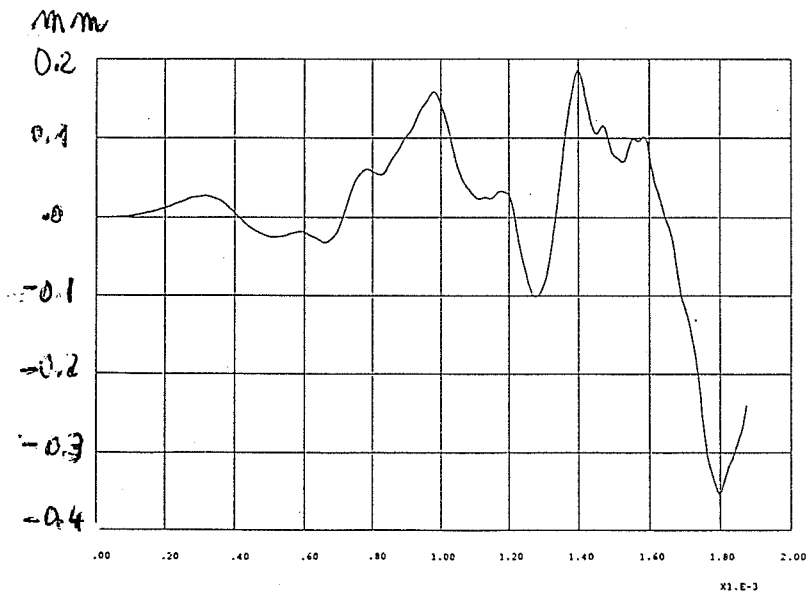


Figure 8 radial displacement on mode 16 for node at 3/4 of height rapid excitation frequency(1500Hz)